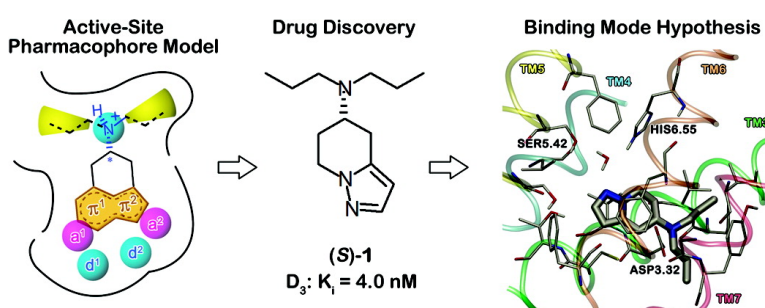


Pharmacophore-Guided Drug Discovery Investigations Leading to Bioactive 5-Aminotetrahydropyrazolopyridines. Implications for the Binding Mode of Heterocyclic Dopamine D₃ Receptor Agonists

Jan Elsner, Frank Boeckler, Frank W. Heinemann, Harald Hbner, and Peter Gmeiner

J. Med. Chem., 2005, 48 (18), 5771-5779 • DOI: 10.1021/jm0503805 • Publication Date (Web): 11 August 2005

Downloaded from <http://pubs.acs.org> on March 28, 2009



More About This Article

Additional resources and features associated with this article are available within the HTML version:

- Supporting Information
- Links to the 3 articles that cite this article, as of the time of this article download
- Access to high resolution figures
- Links to articles and content related to this article
- Copyright permission to reproduce figures and/or text from this article

[View the Full Text HTML](#)

Pharmacophore-Guided Drug Discovery Investigations Leading to Bioactive 5-Aminotetrahydropyrazolopyridines. Implications for the Binding Mode of Heterocyclic Dopamine D3 Receptor Agonists[§]

Jan Elsner,[†] Frank Boeckler,[†] Frank W. Heinemann,[‡] Harald Hübner,[†] and Peter Gmeiner^{*,†}

Department of Medicinal Chemistry, Emil Fischer Center, Friedrich Alexander University, Schuhstrasse 19, D-91052 Erlangen, Germany, and Department of Inorganic Chemistry, Friedrich Alexander University, Egerlandstrasse 1, D-91058 Erlangen, Germany

Received April 22, 2005

Taking advantage of a 3D-QSAR based pharmacophore hypothesis, synthesis and biological evaluation of dopaminergic 5-aminotetrahydropyrazolo[1,5-*a*]pyridines are described. The data displayed substantial and selective D3 receptor affinity for the heterocyclic test compound (\pm)-**1** when the enantiomer (*S*)-**1** turned out to be responsible for the D3 binding ($K_{i \text{ high}} = 4.0 \text{ nM}$). (*S*)-**1** exhibited binding affinity and ligand efficacy comparable to those of our previously described D3 agonist FAUC 54, when subtype selectivity could be significantly improved. The results indicate that the sp^2 nitrogens of the pyrazole and thiazole rings of the dopaminergics (*S*)-**1** and pramipexole, respectively, are pharmacophoric elements of major importance. To provide putative explanations for the high affinity of (*S*)-**1**, computational studies were performed employing an active state D3 model.

Introduction

Dopamine receptors, which belong to the class A rhodopsin-like G protein-coupled receptors, can be divided phylogenetically into D1-like receptors comprising the subtypes D1 and D5 and a D2-like group including D2, D3, and D4.¹ Interestingly, the D3 receptor mRNA has a high abundance in limbic brain areas associated with cognitive and emotional functions² and, therefore, can be considered as particularly related to affective disorders.³ Thus, the D3 receptor has been regarded as an interesting therapeutic target for the treatment of schizophrenia,⁴ Parkinson's disease,⁵ drug-induced dyskinesia,⁶ and cocaine addiction.⁷

Since X-ray crystallographic or nuclear magnetic resonance structural data are not available for any of the aminergic G protein-coupled receptors, we established extensively validated dopamine D2, D3, and D4 receptor models based on the crystal structure of bovine rhodopsin when focusing on the similarity and divergence of the D2-like dopamine receptor subtypes and the respective ligand interactions.^{8,9} As a continuation of these efforts, we were able to transform our homology model of the D3 receptor from an inactive into an active state by employing CoMFA/CoMSIA contribution maps derived from a 3D-QSAR investigation on D3 agonists.¹⁰ Thus, combination of a ligand-based and a structure-based modeling approach yielded a conceptual binding model for D3 agonists, revealing novel insights into the pharmacophoric requirements of potent D3 binding. As depicted and exemplified in the conceptual Figure 1, the essentials of our previous investigations are as follows: (1) All ligands form a reinforced ionic bond (ionic

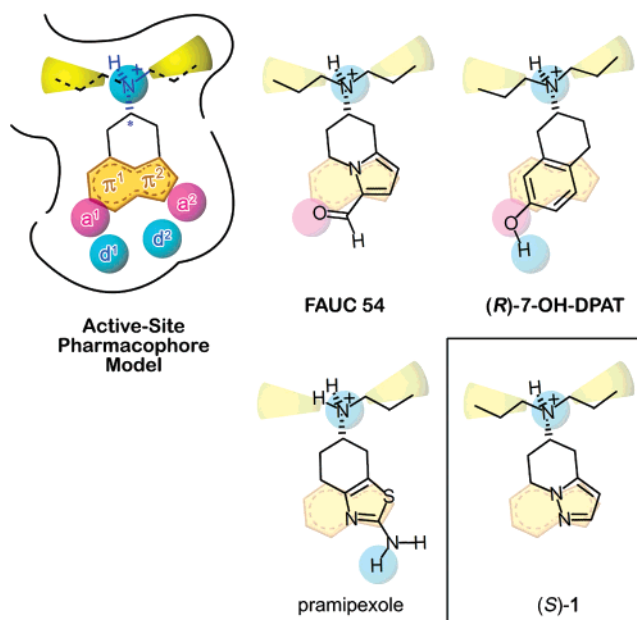


Figure 1. Outline of the ligand design strategy leading to the 5-aminotetrahydropyrazolo[1,5-*a*]pyridine (*S*)-**1** in order to elucidate the significance of the hydrogen-bond acceptor function in pramipexole for D3 receptor recognition. A conceptual pharmacophore model of the D3 receptor active site is illustrated in its general form and exemplified by FAUC 54 and (*R*)-7-OH-DPAT representing the two different classes of stereoisomers. π^1/π^2 (orange indene) indicates the extended aromatic system. Cyan and magenta spheres denote areas where hydrogen-bond donors and acceptors can be located on the ligand site, respectively. The single cyan sphere between the yellow cones marks the hydrogen-bond donor feature of the protonated amine, which is required in each agonist, as it forms a reinforced ionic bond with the highly conserved Asp3.32. The two yellow cones represent the hydrophobic side chains.

interaction enforced by a hydrogen bond) between their protonated amine (cyan sphere) and Asp3.32 within the binding site. (2) The aromatic moieties of the ligands

* To whom correspondence should be addressed. Phone: +49(9131)-8529383. Fax: +49(9131)8522585. E-mail: gmeiner@pharmazie.uni-erlangen.de.

[§] Dedicated to Professor Fritz Eiden on the occasion of his 80th birthday.

[†] Department of Medicinal Chemistry.

[‡] Department of Inorganic Chemistry.

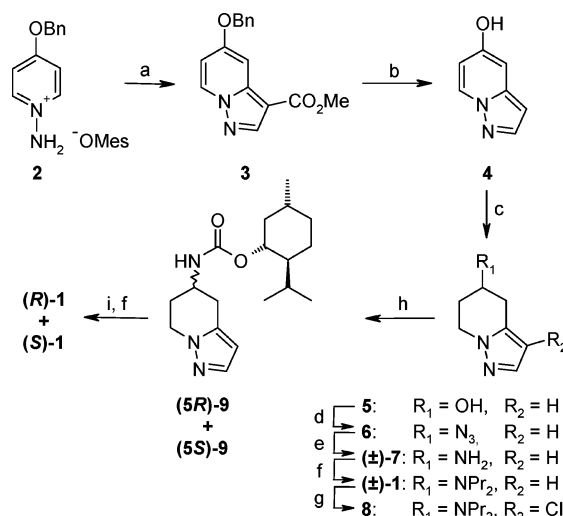
are capable of forming π -stacking interactions with residues of the protein binding pocket within an extended aromatic area (π^1/π^2). The stereochemistry is decisive for the placement of the aromatic moieties when the (*R*)- and (*S*)-configurations lead to a displacement close to π^1 and π^2 , respectively. (3) Substituents at the different aromatic moieties can occupy up to two hydrogen-bond donor (cyan spheres; d¹ and d²) and hydrogen-bond acceptor positions (magenta spheres; a¹ and a²) that are of varying importance. (4) All ligands are anchored with at least one alkyl side chain (yellow cones) in primarily hydrophobic parts of the binding pocket when one of these forms a "propyl-specific" cavity.

Comparing the pK_i values of the 3-formyl substituted 7-aminotetrahydroindolizine FAUC 54 with its 3-unsubstituted congener indicates that occupation of the acceptor position a¹ with the oxygen of the formyl function of FAUC 54 is highly beneficial for D3 receptor binding.^{11,12} Investigation of the D3 agonist (*R*)-7-OH-DPAT facilitates positioning of the oxygen of its 7-hydroxy group onto the pharmacophoric area a¹ when the donor position d¹ is occupied by the OH-hydrogen atom. Based on the high D3 receptor affinities of (*R*)-7-OH-DPAT and FAUC 54, we conclude that the occupation of area a¹ significantly contributes to D3 receptor binding, which is supported by the importance of this area shown in the respective CoMFA and CoMSIA fields. However, as indicated by a simple atom-centered alignment superimposing the core scaffolds of pramipexole¹³ and FAUC 54 (Figure 1), this apparently cannot hold true for a main group of heterocyclic dopaminergics including pramipexole, quinelorane, and quinpirole when area a¹ is not occupied by the endocyclic acceptor functionality. Nevertheless, the exocyclic amino group in position 2 of pramipexole can occupy the area d² and, thus, putatively provides positive contribution to D3 receptor binding. To learn more about the importance of the endocyclic H-bond acceptor at the a¹ site and to exploit this structural element for the discovery of drug-like D3 selective agonists, we were intrigued by the question of whether an unsubstituted pyrazole is sufficient as a bioisosteric subunit. Herein, we report on synthesis, structural elucidation, and pharmacological evaluation of a series of dipropylaminocyclohexene-fused pyrazoles including the tetrahydropyrazolo[1,5-*a*]pyridine (*S*)-**1** and derivatives thereof.

Chemistry

The synthesis of target compounds was performed starting from *N*-amino-4-benzyloxy pyridinium mesitylenesulfonate **2** as a valuable building block that could be prepared by electrophilic amination¹⁴ of 4-benzyloxy pyridine. Subsequent 1,3-dipolar cycloaddition with methyl propiolate under oxidizing conditions afforded the 5-benzyloxy pyrazolo[1,5-*a*]pyridine derivative **3** (Scheme 1). Removal of the carboxylic ester group and cleavage of the benzyl ether function under strong acidic conditions furnished the 5-hydroxypyrazolopyridine **4** in 80% yield,¹⁵ which could be converted to the tetrahydro derivative **5** by catalytic hydrogenation. Whereas all attempts to oxidize the alcohol **5** and introduce the amino function via a reductive amination reaction failed, activation of the alcohol by MsCl followed by nucleophilic substitution with sodium azide gave rise to the

Scheme 1^a



^a Reagents and conditions: (a) methyl propiolate, K₂CO₃, air–O₂, DMF, rt, 16 h (30%); (b) 48% HBr, reflux, 1 h (80%); (c) H₂, Pd/C, EtOH, 20 bar, 80 °C, 16 h (79%); (d) (1) MsCl, Et₃N, THF, –30 °C, 1 h; (2) NaN₃, DMSO, 35 °C, 24 h (45%); (e) H₂, Pd/C, MeOH, rt, 2.5 h (80%); (f) propionaldehyde, NaBH(OAc)₃, 1,2-dichloroethane, rt, 16 h (84–85%); (g) NCS, CHCl₃, reflux, 16 h (67%); (h) (1) (±)-**7**, (–)-menthyl chloroformate, DIPEA, CH₂Cl₂, 0 °C to rt, 16 h (77%); (2) separation of diastereoisomers (31% for each); (i) (1) (CH₃)₃SiI, CHCl₃, reflux, 12 h; (2) MeOH, reflux, 12 h (89%).

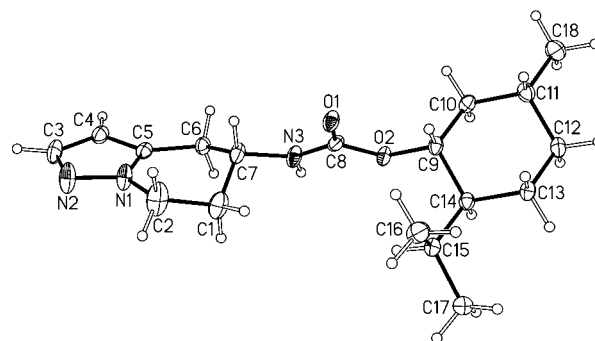
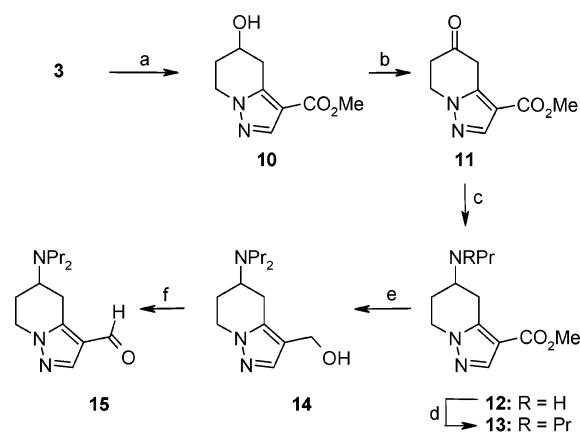


Figure 2. ORTEP drawing of the molecular structure of (–)-menthyl-derived tetrahydropyrazolo[1,5-*a*]pyridine (*5R*)-**9**, determined with X-ray crystallography.

azide **6** in 45% yield. Reduction of the azide functionality afforded the primary amine (±)-**7** followed by reductive alkylation with propionaldehyde furnishing the desired target compound (±)-**1** in racemic form. Treatment of (±)-**1** with *N*-chlorosuccinimide (NCS) in refluxing chloroform proceeded regioselectively, giving access to the 3-chloro derivative **8**.

To investigate the enantiospecificity of the receptor recognition process, racemic (±)-**7** was resolved into its enantiomers. Thus, treatment of (±)-**7** with (–)-menthyl chloroformate gave a mixture of the diastereoisomeric carbamates (*5R*)-**9** and (*5S*)-**9** that could be separated by preparative HPLC. After successful attempts to grow crystals suitable for X-ray analysis of (*5R*)-**9**, which was eluted first, the assignment of the (*R*)-configuration to the newly formed stereogenic center was based on the stereochemical information from the (–)-menthyl group. The X-ray crystal structure of (*5R*)-**9** (Figure 2) clearly indicated that the (–)-menthylcarbonyl moiety adopted an equatorial position. After cleavage of the carbamates (*5R*)-**9** and (*5S*)-**9** by iodotrimethylsilane¹⁶ and subse-

Scheme 2^a

^a Reagents and conditions: (a) H₂, Pd/C, EtOH, 20 bar, 80 °C, 48 h (75%); (b) DMP, CH₂Cl₂, rt, 2 h (70%); (c) propylamine, NaCNBH₃, MeOH, rt, 16 h (60%); (d) propionaldehyde, NaBH(OAc)₃, 1,2-dichloroethane, rt, 16 h (78%); (e) **13**, LiAlH₄, THF, 0 °C to rt, 1.5 h (82%); (f) MnO₂, CH₂Cl₂, rt, 16 h (97%).

quent reductive alkylation of the obtained primary amines (*R*)-**7** and (*S*)-**7**, respectively, with propionaldehyde, the test compounds (*R*)-**1** and (*S*)-**1** could be isolated in enantiomerically pure form.

Besides the 3-chloropyrazolopyridine derivative **8**, we were interested in synthesizing further 3-substituted test compounds taking advantage of the carboxylate function that we introduced in the beginning of the synthesis. Thus, the building block **3** was subjected to a chemoselective hydrogenolytic debenzoylation giving access to the carboxylic ester **10** in 75% yield (Scheme 2). In contrast to the findings observed with the unsubstituted alcohol **5**, oxidation of **10** by using Dess–Martin periodinane (DMP)¹⁷ afforded the ketone **11** in good yield. Subsequent amination and N-alkylation in the presence of NaBH₃CN and NaBH(OAc)₃, respectively, gave access to the mono- and dipropylamines **12** and **13**, respectively. The carboxylic ester function of **13** was reduced with LiAlH₄ to furnish the alcohol **14** and, subsequently, oxidized by MnO₂ to afford the final product **15**.

Results and Discussion

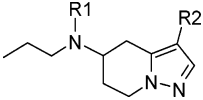
Biological Investigations. Receptor binding experiments were established to evaluate the binding properties of the target compounds (\pm)-**1**, (*R*)-**1**, (*S*)-**1**, **8**, and **12–15** in comparison to the reference FAUC 54 (Table 1). D1 receptor affinities were determined utilizing porcine striatal membranes and the D1 selective radioligand [³H]SCH 23390.¹⁸ D2, D3, and D4 affinities were investigated employing the cloned human dopamine receptors D2_{long}, D2_{short},¹⁹ D3,²⁰ and D4.^{4,21} stably expressed in Chinese hamster ovary cells (CHO) and the radioligand [³H]spiperone.¹⁸ The competition data were analyzed according to a sigmoid model by nonlinear regression. If the dose–response curves showed biphasic properties and the calculated Hill coefficients (n_H) were between -0.50 and -0.75 with a better fit of equation indicating a two-site model and if the amount of calculated high affinity binding sites was greater than 15% of the total receptor population, K_i values for the high and low affinity binding sites of the receptor were derived. The $K_{i\text{ high}}$ values representing the ternary

complex of ligand, receptor, and G-protein thus indicating agonist properties were chosen for the comparison of agonist affinities.

In most cases, the 5-aminotetrahydropyrazolo[1,5-*a*]pyridines investigated displayed only weak to moderate D1 and D2 and D4 binding. However, substantial D3 binding affinity was observed for the heterocyclic target compound (\pm)-**1**. Interestingly, determination of the K_i values of the pure enantiomers revealed that the biological activity is almost exclusively due to (*S*)-**1** ($K_{i\text{ high}} = 4.0$ nM). This finding is in accordance with previously described dopaminergics^{22–25} and our recent observations on aminoindolizines and aminotetrahydroindoles.^{11,26,27} Furthermore, (*S*)-**1** showed substantial D3 subtype selectivity over D2_{long} and D2_{short} and a significant preference when compared to D4. Interestingly, the 3-chloro derivative **8**, which was investigated in racemic form, also exhibited high binding affinity for D3 ($K_{i\text{ high}} = 6.1$ nM) whereas compounds **12–15**, all of which bear larger substituents in position 3, displayed only poor dopamine receptor recognition. To further characterize the binding profiles of (\pm)-**1**, (*R*)-**1**, (*S*)-**1**, **8**, and **12–15**, 5-HT_{1A} and 5-HT₂ affinities were investigated in a screening system with porcine cortical membranes measuring the displacement of the radioligands [³H]8-OH-DPAT and [³H]ketanserin, respectively, by the test compounds at three representative concentrations. All compounds except (*S*)-**1** showed only weak binding at the 5-HT receptors with a capability to displace the radioligand at a concentration of 100 nM with a rate of less than 15%. For (*S*)-**1**, a displacement of 57% for 5-HT_{1A} and 25% for 5-HT₂ indicated a moderate 5-HT affinity. For the most promising compounds (\pm)-**1**, (*R*)-**1**, (*S*)-**1**, and **8**, receptor binding to the porcine α_1 receptor was investigated utilizing the selective radioligand [³H]prazosin when all compounds showed affinities only in the micromolar range.

To investigate the intrinsic activity of the most interesting test compounds (*R*)-**1**, (*S*)-**1**, and **8** compared to FAUC 54 and the reference agonist quinpirole, a mitogenesis assay was performed employing D3 receptor expressing CHO dhfr⁻ cells.^{28,29} Agonist activation of dopamine receptors can be determined by measuring the rate of [³H]thymidine incorporation into growing heterologously transfected cell lines. Intrinsic activities and EC₅₀ values are presented in Table 2 clearly indicating substantial ligand efficacy and potency for (*S*)-**1** (82%, 3.4 nM) and the 3-chloro derivative **8** (54%, 4.5 nM). The obtained data reflect agonist and partial agonist properties of the test compounds when the EC₅₀ values are in good consistence to the $K_{i\text{ high}}$ values derived from the binding experiments.

Theoretical Investigations. To understand the high D3 affinity of the heterocyclic test compounds and to gain more insights into the putative binding modes of pramipexole and (*S*)-**1**, we employed the predictive power of a very recently established 3D-QSAR model for D3 agonists, which has also been used to derive the pharmacophore hypothesis presented in the Introduction.¹⁰ This model was built based on a diverse training set consisting of a series of 34 chiral 7-aminotetrahydroindolizines and 10 commercially available dopaminergics. The PLS analysis of the final CoMFA model revealed a good cross-validated q^2_{cv} of 0.726 ($s_{PRESS} =$

Table 1. Receptor Binding Data of the 5-Amino-4,5,6,7-tetrahydropyrazolo[1,5-*a*]pyridines **1**, **8**, and **12–15** for Human and Porcine Dopamine Receptors^a


compd	R1	R2	K_i (nM) ^a					
			[³ H]SCH23990	[³ H]spiperone				
				pD1	hD2 _{long}	hD2 _{short}	hD3	hD4.4
(±)- 1	Pr	H	high ^b low ^b	>20 000	220 ± 49 18 000 ± 5400	160 ± 45 8500 ± 1300	6.7 ± 1.6 200 ± 21	58 ± 18 1600 ± 910
(<i>R</i>)- 1	Pr	H		>20 000	>20 000	>20 000	2700 ± 760	13 000 ± 3200
(<i>S</i>)- 1	Pr	H	high low	>20 000	180 ± 31 15 000 ± 1500	250 ± 39 10 000 ± 660	4.0 ± 1.3 110 ± 28	58 ± 10 1700 ± 400
8	Pr	Cl	high low	>20 000	120 ± 66 >20 000	210 ± 78 12 000 ± 2600	6.1 ± 1.5 230 ± 32	200 ± 45 6400 ± 1400
12	H	CO ₂ Me		>20 000	>100 000	>100 000	12 000 ± 500	90 000 ± 15 000
13	Pr	CO ₂ Me		>20 000	>20 000	>20 000	17 000 ± 2 500	>20 000
14	Pr	CH ₂ OH		>20 000	>20 000	>20 000	4000 ± 0	16 000 ± 1500
15	Pr	CHO		>20 000	5900 ± 850	4 000 ± 0	12 000 ± 0	14 000 ± 2000
FAUC 54			high low	>20 000 ^c	52 ± 13 6900 ± 1800	41 ± 7.0 3000 ± 170	5.3 ± 1.1 150 ± 16	32 ± 8.5 2500 ± 220
pramipexole			high low	>20 000 ^c	21 ± 4.9 6300 ± 1300	21 ± 5.1 1900 ± 560	0.88 ± 0.15 38 ± 7.0	8.1 ± 1.1 130 ± 22
quinpirole			high low	>20 000 ^c	63 ± 17 3100 ± 800	35 ± 6.0 3000 ± 590	24 ± 6.3 420 ± 140	1.8 ± 0.093 53 ± 5.9

^a K_i values in nM ± SEM are based on the means of 2–7 experiments each done in triplicate. ^b K_i values of the high and low affinity binding state of the receptor when analysis of the binding data resulted in a biphasic dose–response curve. ^c Determined by using bovine D1 receptors.

Table 2. Intrinsic Activity of the Tetrahydropyrazolo[1,5-*a*]pyridines (*R*)-**1**, (*S*)-**1**, **8**, and FAUC 54 Relative to the Reference Compound Quinpirole at the Dopamine D3 Receptor Established by Measuring the Stimulation of Mitogenesis

	test compounds					
	(<i>S</i>)- 1	(<i>R</i>)- 1	8	FAUC 54	quinpirole	pramipexole
ligand efficacy ^a	82%	n.e. ^b	54%	86%	100%	93%
EC ₅₀ (nM) ^c	3.4	4.5	1.1	2.6	1.5	1.5

^a Rate of incorporation of [³H]thymidine (in %) as evidence for a mitogenetic activity relative to the full agonist effect of quinpirole (100%) as the mean value of quadruplicates from 2 to 8 experiments. ^b No effect. ^c EC₅₀ values are derived from the mean curves of the experiments.

Table 3. Prediction of Binding Affinities for Pramipexole and (*S*)-**1** in Three Different Alignments Employing an Established CoMFA Model of D3 Agonists

alignment	pramipexole		(S)- 1		
	pK _i	ΔpK _i	pK _i	ΔpK _i	
experiment	9.06		8.40		
prediction	π ²	7.45	−1.61	6.52	−1.88
prediction	π ¹	8.90	−0.16	7.30	−1.10
prediction	π ² + H ₂ O	8.60	−0.46	7.68	−0.72

0.719) at an optimum of five components. To obtain completely unbiased predictions, we removed pramipexole from the training set, decreasing the cross-validated q^2_{cv} only marginally ($q^2_{cv} = 0.700$).

Following our initial alignment defined by an atom-based superimposition of the core scaffold of pramipexole or (*S*)-**1** on FAUC 54, we discovered a substantial underestimation of the predicted binding affinities by 1.61 and 1.88 pK_i units for pramipexole and (*S*)-**1**, respectively (Table 3). These prediction errors exceeded by far the values as expected on the basis of the s_{PRESS} value of the CoMFA model reflecting that the initial π² alignment of neither pramipexole nor (*S*)-**1** represents

a putative binding mode that yields a satisfying explanation of the corresponding D3 affinity.

Application of a similarity-based algorithm led to an alternative alignment of pramipexole displacing the thiazole ring from π² toward π¹ (Figure 3)¹⁰ when the heterocyclic sp² nitrogen is closely approaching a¹ and the amino hydrogens can occupy at least one of the donor areas d¹ and d². However, this modified alignment is formed at the cost of a less precise match of the protonated amine and the propyl side chain with their pharmacophoric areas. Interestingly, the D3 affinity of (*S*)-**1** was still underestimated (1.10 pK_i units) when the QSAR-derived π¹ alignment of pramipexole was transferred to (*S*)-**1**. Considering the inability to predict (*S*)-**1** correctly and the disputable issue concerning the orientation and placement of the side chain within the propyl-specific receptor cavity, we continued to search for a binding mode that allows reasonably good predictions for both investigated ligands. We found such an alternative explanation of the binding properties by taking into consideration that the ligands may potentially bind to the receptor through a mediated interaction. We were intrigued by the question of whether we could find indications supporting that water participates in the receptor binding of (*S*)-**1** and pramipexole. Our hypothesis was inspired by recent investigations,³⁰ reporting a paradigm of a drug design-relevant mediation of ligand–protein interactions between the enzyme tRNA-guanine transglycosylase and a novel inhibitor by a water molecule. It is interesting to note that ligands with a pyrazole partial structure are described to stably interact with a protein through an associated water (PDB code: 1UDT, sildenafil–PDE5 complex).³¹ Moreover, several crystal structures of bovine rhodopsin (PDB code: 1L9H, 1GZM, and 1U19),^{32–34} which is the only G protein-coupled receptor successfully crystallized

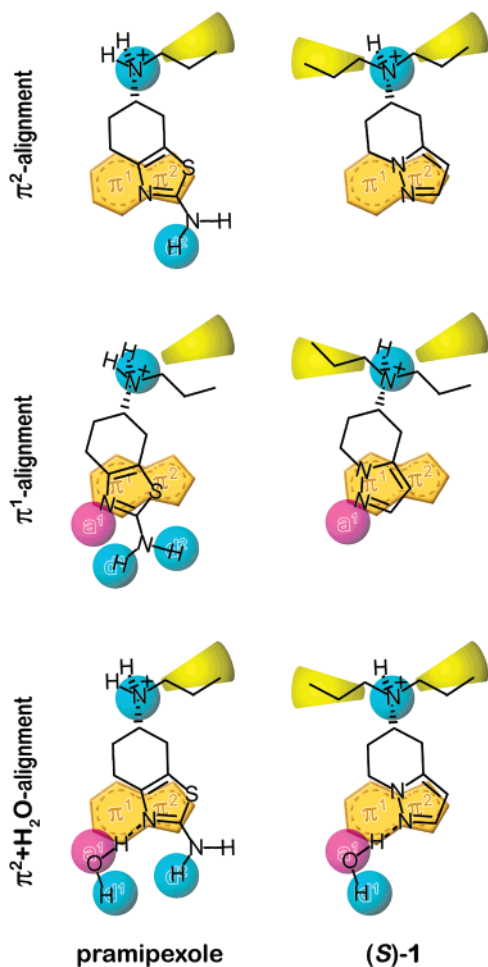


Figure 3. Depiction of the three different alignment modes of pramipexole and (*S*)-1, which were evaluated by the prediction of their corresponding pK_i values employing the previously established 3D-QSAR model. The π^2 alignment is generated by a simple atom-based superimposition of the aromatic moieties on π^2 , while the π^1 alignment evolved from a similarity based repositioning of pramipexole on pergolide as performed in the original QSAR investigation. The $\pi^2 + \text{H}_2\text{O}$ alignment reflects the addition of a water molecule mediating the hydrogen-bonding interactions between the ligand and the receptor.

up to date, display water in hydrophilic regions of the binding pocket.

To characterize the bonding geometry and quantify the energy of water attached to the 5-aminotetrahydropyrazolo[1,5-*a*]pyridine substructure of (*S*)-1 relative to other standard ligands, we utilized a validated quantum mechanical approach established by Rablen et al.³⁵ Our calculations yield a distance of 1.94 Å between the sp^2 hybridized pyrazole nitrogen and one of the water hydrogens, which is in the typical range for a hydrogen-bonding interaction. The related bonding angle toward the water oxygen ($\text{N}-\text{H}\cdots\text{O}$) only deviated by 14.3° from the ideal linear arrangement. The interaction energy of $-\Delta E = 7.24$ kcal/mol lies in the top range of all the comparative values published in the original investigation, in general, and of the interaction energies with sp^3/sp^2 nitrogens as acceptors, in particular. For instance, the bonding energy for an imidazole system (sp^2 N as acceptor) falls short by approximately 0.6 kcal/mol ($-\Delta E = 6.68$ kcal/mol) and for pyridine by almost 1 kcal/mol ($-\Delta E = 6.26$ kcal/mol).

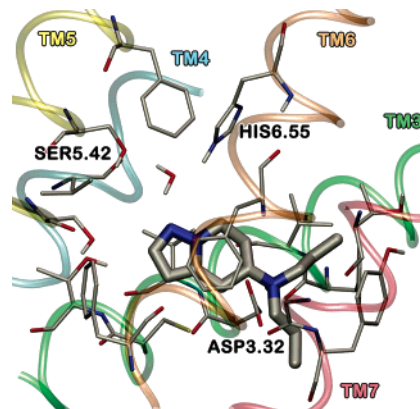


Figure 4. Depiction of the water-mediated ligand–receptor complex of (*S*)-1 and the “active-state” D3 receptor. The transmembrane helices (TM3 to TM7) are shown for better orientation as uniquely colored transparent tubes. The picture was prepared with VMD1.8.2.

Based on these theoretical calculations, a water-mediated ligand–receptor interaction appears to be feasible for (*S*)-1. Thus, we decided to include a ligand-associated water molecule in the CoMFA predictions applying the geometry of the bound water as obtained from DFT calculations. As given in Table 3, the pK_i value of (*S*)-1 for this was improved by 1.16 units and 0.38 unit compared to the pure π^2 and π^1 alignments, respectively, and deviates by 0.72 unit from the experimental value. Additionally, a reasonable precision of the pK_i prediction (deviation: 0.46 pK_i unit) was achieved for the corresponding complex of pramipexole with water. Obviously, the relative disposition of the oxygen function and the electrostatic and steric requirements are crucial to the binding energy, since (*S*)-3-hydroxymethyl-7-dipropylamino-5,6,7,8-tetrahydroindolizine displayed only a pK_i of 6.38,¹¹ reflecting that a hydroxymethyl group is not able to simulate the water mediation. Interestingly, this could be also predicted by our CoMFA displaying a calculated pK_i of 6.49 when employing a minimal energy conformation with an orientation of the hydroxymethyl group similar to the $\pi^2 + \text{H}_2\text{O}$ complex of (*S*)-1. Consequently, the concept of a water-mediated ligand–receptor interaction seems to be a plausible alternative, as it yields satisfying predictions in the range of the CoMFA s_{PRESS} value for both compounds. However, it should be recalled that various enthalpy or entropy related effects contribute to the total binding energy and, thus, other explanations which may be not determinable with the CoMFA-methodology could also be responsible for the high D3 binding of (*S*)-1 or pramipexole. For instance, the modified π -stacking interaction of the pyrazole moiety of (*S*)-1 as compared to the formyl substituted pyrrole partial structure of FAUC 54 could be relevant for the binding energy, as similarly suggested for a series of heteroaromatic hSST4 receptor ligands.³⁶

Based on the alignment of the water–(*S*)-1 complex with the QSAR dataset, as used for the prediction of the binding affinity, we visualized and examined the putative interactions between (*S*)-1, water, and the D3 receptor on a molecular level in this active-state model (Figure 4). The ligand binds as expected through a reinforced ionic bond with its protonated amine to Asp3.32, which is completely conserved among biogenic

amine GPCRs. Beyond its hydrogen bond to the pyrazole nitrogen, the interstitial water can putatively form two other hydrogen bonds. On one hand, the oxygen can accept a hydrogen bond from His6.55, and on the other hand, the free hydrogen can donate one to Ser5.42. Thus, we can assume that the interstitial water is able to mediate the binding between the ligand and up to two residues in TM5 and TM6, alternatively or simultaneously. Consequently, it appears to be also reasonable on the level of molecular interactions that appending a single water molecule to the ligand–receptor complex can significantly contribute to the high D3 binding affinity of (*S*)-**1**, as the lack of interaction feasibility of the regionally restricted acceptor system in (*S*)-**1** is compensated.

In accordance with earlier studies,³⁷ residues that differ between the D3 and D2 receptors being also located closely to the putative agonist binding site and, thus, possibly responsible for inducing the D3 receptor preference of (*S*)-**1** could not be identified.

Conclusions

Employing a 3D-QSAR derived pharmacophore hypothesis for the design of dopamine D3 receptor agonists, a series of novel 5-aminotetrahydropyrazolo[1,5-*a*]pyridines was synthesized and evaluated in vitro for dopamine receptor affinity and ligand efficacy. The results showed substantial and selective D3 receptor affinity for the heterocyclic test compound (\pm)-**1** when the enantiomer (*S*)-**1** turned out to be exclusively responsible for the D3 binding. The low nanomolar $K_{i \text{ high}}$ value for the D3 affinity of (*S*)-**1** (4.0 nM) indicates that the sp^2 nitrogens of the pyrazole and thiazole rings of the dopaminergics (*S*)-**1** and pramipexole, respectively, are pharmacophoric elements of major importance. Based on our computational investigations, the interactions between the endocyclic nitrogen of the heteroarene subunit and the receptor may be mediated by an interstitial water molecule.

Experimental Section

Chemistry. All reactions were carried out under nitrogen atmosphere except 1,3-dipolar cycloadditions, ester hydrolyses, and catalytic hydrogenations. Solvents were purified and dried by standard procedures. All reagents were of commercial quality and used as purchased. MS were run on a Finnegan MAT TSQ 70 spectrometer by EI (70 eV) with solid inlet. α^{20}_D values were measured on a Perkin-Elmer 241 instrument. The ^1H NMR spectra were obtained on a Bruker AM 360 (360 MHz) spectrometer, if not otherwise stated in CDCl_3 relative to TMS (J values in Hz). IR spectra were performed on a Jasco FT/IR 410 spectrometer. Purification by chromatography was performed using Silica Gel 60; TLC analyses were performed using Merck 60 F₂₅₄ aluminum sheets and analyzed by UV light (254 nm) or in the presence of iodine. Preparative and analytical HPLC was performed on an Agilent 1100 preparative HPLC system employing a VWL detector. CHN elementary analyses were performed at the Department of Organic Chemistry of the Friedrich Alexander University.

Methyl 5-Benzoyloxy-pyrazolo[1,5-*a*]pyridine-3-carboxylate (3). To an ice-cooled solution of 4-benzoyloxy-pyridine (13.8 g; 74.5 mmol) in CH_2Cl_2 (75 mL) was added dropwise a solution of *O*-mesitylenesulfonylhydroxylamine (90% purity; 17.8 g; 74.5 mmol) in CH_2Cl_2 (75 mL). The reaction mixture was stirred at 0 °C for 1 h and at room temperature for 1 h. After the addition of Et_2O , the separated oil was washed with Et_2O and dried under reduced pressure. The crude product (**2**) was dissolved in DMF (100 mL). After the addition of K_2CO_3 (13.7

g; 99 mmol) and methyl propiolate (6.1 g; 72.5 mmol), the reaction mixture was stirred vigorously at room temperature overnight. The precipitate was filtered, and the filtrate was concentrated. The residue was treated with a saturated NaHCO_3 solution and extracted with CH_2Cl_2 . The organic layer was washed with 1 N HCl and H_2O , dried, and evaporated. Flash chromatography (hexanes– EtOAc 9:1) yielded **3** (6.3 g; 30%) as a pale yellow oil: ^1H NMR δ 3.90 (s, 3H), 5.17 (s, 2H), 6.68 (dd, $J = 7.5$ Hz, 2.1 Hz, 1H), 7.35–7.50 (m, 5H), 7.53 (d, $J = 2.1$ Hz, 1H), 8.28 (s, 1H), 8.34 (br d, $J = 7.5$ Hz, 1H); EIMS 282 (M^+). Anal. ($\text{C}_{16}\text{H}_{14}\text{N}_2\text{O}_3$) C, H, N.

5-Hydroxypyrazolo[1,5-*a*]pyridine (4). A mixture of **3** (5.00 g, 17.7 mmol) and 48% HBr (60 mL) was refluxed for 1 h. The cooled solution was neutralized (2 N NaOH, NaHCO_3) and extracted with Et_2O . The organic layer was dried and evaporated, and the residue was purified by flash chromatography (hexanes– EtOAc 1:1) to give **4** (1.9 g, 80%) as a pale yellow solid; for experimental data, see ref 15.

4,5,6,7-Tetrahydropyrazolo[1,5-*a*]pyridin-5-ol (5). To a solution of **4** (1 g; 7.46 mmol) in EtOH (20 mL) was added 10% Pd/C (220 mg). The mixture was stirred under 20 bar of hydrogen and at 80 °C for 16 h. The mixture was filtered, and the filtrate was evaporated. The residue was purified by flash chromatography (hexanes– EtOAc 2:3) to afford **5** (814 mg (79%)) as a colorless oil: ^1H NMR δ 2.10–2.25 (m, 2H), 2.83 (dd, $J = 16.3$ Hz, 6.4 Hz, 1H), 3.10 (dd, $J = 16.3$ Hz, 4.6 Hz, 1H), 4.13–4.20 (m, 1H), 4.29–4.37 (m, 2H), 6.01 (d, $J = 1.8$ Hz, 1H), 7.44 (d, $J = 1.8$ Hz, 1H); EIMS 138 (M^+). Anal. ($\text{C}_7\text{H}_{10}\text{N}_2\text{O}$) C, H, N.

5-Azido-4,5,6,7-tetrahydropyrazolo[1,5-*a*]pyridine (6). Et_3N (327 mg, 3.24 mmol) and MsCl (399 mg, 3.51 mmol) were added to a solution of **5** (404 mg, 2.93 mmol) in THF (25 mL) at –30 °C. After 1 h, the precipitate was filtered and the filtrate was evaporated without heating. The residue was dissolved in DMSO (25 mL), NaN_3 (981 mg, 15.1 mmol) was added, and the reaction mixture was stirred at 35 °C for 24 h. After the addition of saturated NaHCO_3 solution, the mixture was extracted with Et_2O and washed thoroughly with brine. The organic layer was dried (Na_2SO_4) and evaporated, and the residue was purified by flash chromatography (hexanes– EtOAc 4:1) to give **6** (214 mg, 45%) as a colorless oil: ^1H NMR δ 2.14–2.33 (m, 2H), 2.90 (dd, $J = 16.7$ Hz, 6.9 Hz, 1H), 3.14 (dd, $J = 16.7$ Hz, 5.0 Hz, 1H), 4.07–4.01 (m, 1H), 4.15–4.23 (m, 1H), 4.27–4.37 (m, 1H), 6.04 (d, $J = 1.8$ Hz, 1H), 7.47 (d, $J = 1.8$ Hz, 1H); EIMS 163 (M^+). Anal. ($\text{C}_7\text{H}_{11}\text{N}_5$) C, H, N.

5-Amino-4,5,6,7-tetrahydropyrazolo[1,5-*a*]pyridine (\pm)-7). A mixture of **6** (200 mg, 1.23 mmol) and 10% Pd/C (100 mg) in MeOH was stirred under a balloon of H_2 at room temperature for 2.5 h. The mixture was filtered through Celite, the filtrate was evaporated carefully, and the residue was purified by flash chromatography (CH_2Cl_2 –MeOH 4:1) to give (\pm)-**7** (134 mg, 80%) as a colorless oil: ^1H NMR δ 1.88–1.99 (m, 1H), 2.13–2.21 (m, 1H), 2.55 (dd, $J = 16.1$ Hz, 8.8 Hz, 1H), 3.08 (dd, $J = 16.1$ Hz, 5.1 Hz, 1H), 3.35 (dddd, $J = 9.7$ Hz, 8.8 Hz, 5.1 Hz, 3.0 Hz, 1H), 4.12 (ddd, $J = 12.9$ Hz, 10.0 Hz, 5.2 Hz, 1H), 4.34 (ddd, $J = 12.9$ Hz, 5.6 Hz, 4.5 Hz, 1H), 5.99 (br d, $J = 1.8$ Hz, 1H), 7.45 (d, $J = 1.8$ Hz, 1H); EIMS 137 (M^+). Anal. ($\text{C}_7\text{H}_{11}\text{N}_3$) C, H, N.

5-Dipropylamino-4,5,6,7-tetrahydropyrazolo[1,5-*a*]pyridine (\pm)-1. To a solution of (\pm)-**7** (20 mg, 0.15 mmol) in 1,2-dichloroethane (3 mL) were added propionaldehyde (17.6 mg, 0.31 mmol) and $\text{Na}(\text{OAc})_3\text{BH}$ (81.4 mg, 0.39 mmol), and the reaction mixture was stirred at room temperature for 16 h. After the addition of saturated NaHCO_3 solution, the organic layer was separated and the aqueous layer was extracted twice with CH_2Cl_2 . The combined organic layers were dried (Na_2SO_4) and evaporated, and the residue was purified by flash chromatography (CH_2Cl_2 –MeOH 19:1) to give (\pm)-**1** (27 mg, 84%) as a colorless oil: ^1H NMR δ 0.89 (t, $J = 7.4$ Hz, 6H), 1.41–1.51 (m, 4H), 1.91–2.03 (m, 1H), 2.11–2.18 (m, 1H), 2.46 (t, $J = 7.4$ Hz, 4H), 2.67 (dd, $J = 16.0$ Hz, 11.2 Hz, 1H), 2.96 (dd, $J = 16.0$ Hz, 4.9 Hz, 1H), 3.03–3.12 (m, 1H), 4.04 (ddd, $J = 12.7$ Hz, 12.4 Hz, 4.7 Hz, 1H), 4.38 (ddd, $J = 12.7$ Hz, 5.7

Hz, 2.3 Hz, 1H), 5.96 (br d, $J = 1.8$ Hz, 1H), 7.42 (d, $J = 1.8$ Hz, 1H); EIMS 221 (M^+). Anal. ($C_{13}H_{23}N_3$) C, H, N.

2-Chloro-5-dipropylamino-4,5,6,7-tetrahydropyrazolo[1,5-a]pyridine (8). A mixture of (\pm)-**1** (12.7 mg, 0.06 mmol) and *N*-chlorosuccinimide (15.3 mg, 0.12 mmol) in CH_2Cl_2 (4 mL) was refluxed for 16 h. The solvent was evaporated, and the residue was purified by flash chromatography (CH_2Cl_2 -MeOH 19:1) to give **8** (10 mg, 67%) as a pale yellow oil: 1H NMR δ 0.89 (t, $J = 7.4$ Hz, 6H), 1.41–1.51 (m, 4H), 1.91–2.02 (m, 1H), 2.10–2.17 (m, 1H), 2.47 (t, $J = 7.4$ Hz, 4H), 2.54 (dd, $J = 16.3$ Hz, 10.7 Hz, 1H), 2.90 (dd, $J = 16.3$ Hz, 5.0 Hz, 1H), 3.04–3.12 (dddd, m, 1H), 4.02 (ddd, $J = 12.7$ Hz, 12.3 Hz, 4.6 Hz, 1H), 4.02 (ddd, $J = 12.7$ Hz, 5.4 Hz, 2.3 Hz, 1H), 7.37 (s, 1H); EIMS 255 (M^+). Anal. ($C_{13}H_{22}N_3$) C, H, N.

(1*R*,2*S*,5*R*)-Menthyl *N*-(4,5,6,7-tetrahydropyrazolo[1,5-a]pyrid-5-yl)-carbamate (9). To a solution of (\pm)-**7** (110 mg, 0.80 mmol) and diisopropylethylamine (156 mg, 1.21 mmol) in CH_2Cl_2 (3 mL) was added slowly (1*R*,2*S*,5*R*)-(-)-menthyl chloroformate (265 mg, 1.21 mmol) at 0 °C. The mixture was stirred at room temperature for 16 h. After the addition of saturated $NaHCO_3$ solution, the organic layer was separated and the aqueous layer was extracted thrice with CH_2Cl_2 . The combined organic layers were dried (Na_2SO_4) and evaporated, and the residue was purified by flash chromatography (CH_2Cl_2 -MeOH 97:3) to afford a diastereomeric mixture of **9** (197 mg, 77%) as colorless crystals.

The diastereoisomers were separated by preparative HPLC using a normal phase column (Luna 5 μ m silica). The mobile phase used was 15% acetonitrile in diisopropyl ether with a flow rate of 21.2 mL/min. The two fractions were eluted with retention times of 17.20 min for the (5*R*)-isomer ((5*R*)-**9**) and 18.30 min for the (5*S*)-isomer ((5*S*)-**9**). Final purity of the separated diastereoisomers was checked by an analytical normal phase column (Luna 5 μ m silica) using the same mobile phase with a flow rate of 1 mL/min. Pure diastereomers (5*R*)-**9** and (5*S*)-**9** were eluted at 15.87 and 16.96 min, respectively. Compound (5*R*)-**9** was isolated (80 mg, 31%) as colorless crystals: 1H NMR δ 0.79–0.97 (m, 10 H), 1.03–1.10 (m, 1H), 1.27–1.69 (m, 5H), 1.86–1.91 (m, 1H), 2.02–2.06 (m, 1H), 2.09–2.16 (m, 1H), 2.24–2.29 (m, 1H), 2.70 (dd, $J = 16.2$ Hz, 7.6 Hz, 1H), 3.19 (dd, $J = 16.2$ Hz, 4.9 Hz, 1H), 4.14 (br s, 1H), 4.19–4.28 (m, 2H), 4.57–4.66 (m, 2H), 6.01 (br d, $J = 1.9$ Hz, 1H), 7.46 (d, $J = 1.9$ Hz, 1H); EIMS 319 (M^+). Anal. ($C_{18}H_{29}N_3O_2$) C, H, N. Compound (5*S*)-**9** was isolated (80 mg, 31%) as colorless crystals.

(*R*)-5-Amino-4,5,6,7-tetrahydropyrazolo[1,5-a]pyridine (*R*)-7. To a solution of (5*R*)-**9** (70 mg, 0.22 mmol) in $CHCl_3$ (3 mL) was added iodotrimethylsilane (188 mg, 0.94 mmol), and the reaction mixture was refluxed for 12 h. After cooling to room temperature, the mixture was treated with MeOH (3 mL) and refluxed for an additional 12 h. The solvent was evaporated, and the residue was purified by flash chromatography (CH_2Cl_2 -MeOH 4:1) to give (*R*)-**7** (27 mg, 89%) as a colorless oil: $[\alpha]^{20}_D = +55.7^\circ$ ($c = 0.5$, $CHCl_3$). (*S*)-**7** (26 mg, 87%) ($[\alpha]^{20}_D = -55.4^\circ$ ($c = 0.5$, $CHCl_3$)) was prepared from (5*S*)-**9** as described above for (*R*)-**7**.

(*R*)-5-Dipropylamino-4,5,6,7-tetrahydropyrazolo[1,5-a]pyridine ((*R*)-1). (*R*)-**1** (20.6 mg, 85%) was prepared as described for (\pm)-**1** using (*R*)-**7** (15 mg, 0.11 mmol) in 2 mL of 1,2-dichloroethane, propionaldehyde (13.2 mg, 0.23 mmol), and $Na(OAc)_3BH$ (61.1 mg, 0.29 mmol): $[\alpha] = +25.2^\circ$ ($c = 0.3$, $CHCl_3$). (*S*)-**1** (19.4 mg, 80%) ($[\alpha]^{20}_D = -25^\circ$ ($c = 0.3$, $CHCl_3$)) was prepared from (*S*)-**7** as described above for (*R*)-**1**.

Methyl 5-Hydroxy-4,5,6,7-tetrahydropyrazolo[1,5-a]pyridine-3-carboxylate (10). To a solution of **3** (850 mg; 3.01 mmol) in EtOH (12 mL) was added 10% Pd/C (200 mg). The mixture was hydrogenated in an autoclave under 20 bar of hydrogen at 80 °C for 48 h. The mixture was filtered, and the filtrate was evaporated. The residue was purified by flash chromatography (hexanes-EtOAc 1:1) to afford **10** (443 mg, 75%) as a pale yellow oil: 1H NMR δ 2.29–2.42 (m, 2H), 2.82 (dd, $J = 17.0$ Hz, 9.6 Hz, 1H), 3.66 (dd, $J = 17.0$ Hz, 5.3 Hz, 1H), 3.81 (s, 3H), 4.05–4.34 (m, 3H), 7.89 (s, 1H); EIMS 196 (M^+). Anal. ($C_9H_{12}N_2O_3$) C, H, N.

Methyl 5-Oxo-4,5,6,7-tetrahydropyrazolo[1,5-a]pyridine-3-carboxylate (11). To a solution of **10** (161 mg, 0.82 mmol) in CH_2Cl_2 (10 mL) was added a solution of DMP (Dess–Martin periodinane; 452 mg; 1.07 mmol) at room temperature. After 2 h, an aqueous $NaHCO_3/Na_2S_2O_3$ solution (1:1) and Et_2O (100 mL) were added and stirring was continued for 10 min. The organic layer was separated, and the aqueous layer was extracted twice with Et_2O . The combined organic layers were dried (Na_2SO_4) and evaporated, and the residue was purified by flash chromatography (hexanes-EtOAc 9:1) to give **11** (112 mg, 70%) as a pale reddish oil: 1H NMR δ 2.91 (t, $J = 6.4$ Hz, 2H), 3.83 (s, 3H), 4.00 (s, 2H), 4.55 (t, $J = 6.4$ Hz, 2H), 7.92 (s, 1H); EIMS 194 (M^+). Anal. ($C_9H_{10}N_2O_3$) C, H, N.

Methyl 5-Propylamino-4,5,6,7-tetrahydropyrazolo[1,5-a]pyridine-3-carboxylate (12). To a solution of **11** (60 mg, 0.31 mmol) in MeOH (6 mL) were added propylamine (21.6 mg, 0.37 mmol) and $NaCNBH_3$ (38.8 mg, 0.62 mmol), and the reaction mixture was stirred at room temperature for 16 h. After the addition of 1 N HCl, saturated $NaHCO_3$ solution and Et_2O were added. The organic layer was dried (Na_2SO_4) and evaporated, and the residue was purified by flash chromatography (CH_2Cl_2 -MeOH 19:1) to give **12** (44 mg, 60%) as a colorless oil: 1H NMR δ 0.94 (t, $J = 7.5$ Hz, 3H), 1.47–1.58 (m, 2H), 1.91–2.01 (m, 1H), 2.15–2.23 (m, 1H), 2.67 (t, $J = 6.7$ Hz, 2H), 2.79 (dd, $J = 17.4$ Hz, 7.8 Hz, 1H), 3.09–3.16 (m, 1H), 3.40 (dd, $J = 17.4$ Hz, 5.0 Hz, 1H), 3.81 (s, 3H), 4.12 (ddd, $J = 13.0$ Hz, 8.8 Hz, 4.9 Hz, 1H), 4.32 (ddd, $J = 13.0$ Hz, 5.4 Hz, 5.2 Hz, 1H), 7.86 (s, 1H); EIMS 237 (M^+). Anal. ($C_{12}H_{19}N_3O_2$) C, H, N.

Methyl 5-Dipropylamino-4,5,6,7-tetrahydropyrazolo[1,5-a]pyridine-3-carboxylate (13). To a solution of **12** (29.9 mg, 0.13 mmol) in 1,2-dichloroethane (3 mL) were added propionaldehyde (8.7 mg, 0.15 mmol) and $Na(OAc)_3BH$ (48 mg, 0.23 mmol), and the reaction mixture was stirred at room temperature for 16 h. After the addition of saturated $NaHCO_3$ solution, the organic layer was separated and the aqueous layer was extracted twice with CH_2Cl_2 . The combined organic layers were dried (Na_2SO_4) and evaporated, and the residue was purified by flash chromatography (CH_2Cl_2 -MeOH 19:1) to give **13** (27.5 mg, 78%) as a colorless oil: 1H NMR δ 0.89 (t, $J = 7.5$ Hz, 6H), 1.41–1.51 (m, 4H), 1.93–2.05 (m, 1H), 2.12–2.19 (m, 1H), 2.48 (t, $J = 7.3$ Hz, 4H), 2.81 (dd, $J = 17.4$ Hz, 11.7 Hz, 1H), 3.06–3.14 (m, 1H), 3.35 (dd, $J = 17.4$ Hz, 5.0 Hz, 1H), 3.81 (s, 3H), 4.08 (ddd, $J = 13.0$ Hz, 12.3 Hz, 4.7 Hz, 1H), 4.37 (ddd, $J = 13.0$ Hz, 5.5 Hz, 2.5 Hz, 1H), 7.85 (s, 1H); EIMS 279 (M^+). Anal. ($C_{15}H_{25}N_3O_2$) C, H, N.

(5-Dipropylamino-4,5,6,7-tetrahydropyrazolo[1,5-a]pyrid-3-yl)-methanol (14). A solution of **13** (20 mg; 0.072 mmol) in THF (2 mL) was treated with $LiAlH_4$ (1 M in THF, 72 μ L, 0.072 mmol) at room temperature and stirred for 1.5 h. After the addition of 0.2 mL of H_2O , the suspension was filtered and washed with Et_2O . The organic layer was dried (Na_2SO_4) and evaporated, and the residue was purified by flash chromatography (CH_2Cl_2 -MeOH 9:1) to give **14** (15 mg, 82%) as a colorless oil: 1H NMR δ 0.89 (t, $J = 7.5$ Hz, 6H), 1.41–1.51 (m, 4H), 1.91–2.03 (m, 1H), 2.11–2.18 (m, 1H), 2.47 (t, $J = 7.5$ Hz, 4H), 2.64 (dd, $J = 16.0$ Hz, 11.4 Hz, 1H), 3.00 (dd, $J = 16.0$ Hz, 5.0 Hz, 1H), 3.05–3.13 (m, 1H), 4.04 (ddd, $J = 12.8$ Hz, 12.4 Hz, 4.6 Hz, 1H), 4.36 (ddd, $J = 12.8$ Hz, 5.7 Hz, 2.1 Hz, 1H), 4.51 (d, $J = 3.2$ Hz, 2H), 7.44 (s, 1H); EIMS 251 (M^+). Anal. ($C_{14}H_{25}N_3O$) C, H, N.

5-Dipropylamino-4,5,6,7-tetrahydropyrazolo[1,5-a]pyridine-3-carbaldehyde (15). To a solution of **14** (12 mg, 0.048 mmol) in CH_2Cl_2 (2 mL) was added MnO_2 (42.5 mg, 0.49 mmol), and the reaction mixture was stirred at room temperature for 16 h. The suspension was filtered, and the filtrate was evaporated. Flash chromatography (CH_2Cl_2 -MeOH 95:5) yielded **15** (11.5 mg, 97%) as a pale yellow oil: 1H NMR δ 0.89 (t, $J = 7.5$ Hz, 6H), 1.41–1.51 (m, 4H), 1.98–2.09 (m, 1H), 2.14–2.21 (m, 1H), 2.47 (t, $J = 7.5$ Hz, 4H), 2.88 (dd, $J = 17.4$ Hz, 10.6 Hz, 1H), 3.09–3.17 (m, 1H), 3.34 (dd, $J = 17.4$ Hz, 5.0 Hz, 1H), 4.11 (ddd, $J = 13.3$ Hz, 12.5 Hz, 4.5 Hz, 1H), 4.39 (ddd, $J = 13.3$ Hz, 5.5 Hz, 2.5 Hz, 1H), 7.88 (s, 1H), 9.85 (s, 1H); EIMS 249 (M^+). Anal. ($C_{14}H_{23}N_3O$) C, H, N.

Dopamine Receptor Binding Studies. Receptor binding studies were carried out as described.¹⁸ In brief, the dopamine D1 receptor assay was done with porcine striatal membranes at a final protein concentration of 40 $\mu\text{g}/\text{assay tube}$ and the radioligand [³H]SCH 23390 at 0.3 nM ($K_d = 0.62\text{--}0.95$ nM). Competition experiments with the human D2_{long}, D2_{short}, D3, and D4.4 receptors were run with preparations of membranes from CHO cells stably expressing the corresponding receptor and [³H]spiperone at a final concentration of 0.5 nM. The assays were carried out with a protein concentration of 5–20 $\mu\text{g}/\text{assay tube}$ and K_d values of 0.06–0.14 nM, 0.09–0.15 nM, 0.08–0.35 nM, and 0.15–0.40 nM for the D2_{long}, D2_{short}, D3, and D4.4 receptors, respectively. Protein concentration was established by the method of Lowry using bovine serum albumin as standard.³⁸

5-HT and $\alpha 1$ Receptor Binding Studies. Receptor binding experiments were performed with homogenates prepared from porcine cerebral cortex as described.³⁹ Assays were run with membranes at a protein concentration per each assay tube of 100, 80, and 60 $\mu\text{g}/\text{mL}$ for 5-HT1_A, 5-HT2, and $\alpha 1$ receptor, respectively, and K_d values of 2.3 nM for 5-HT1_A, 1.7 nM for 5-HT2, and 0.05–0.10 nM for the $\alpha 1$ receptor. A screening system was established to investigate serotonin receptor binding when measuring the displacement of the radioligands [³H]8-OH-DPAT and [³H]ketanserin (each at a final concentration of 0.5 nM) from 5-HT1_A and 5-HT2 carrying membranes by the test compounds at final concentrations of 10 μM , 100 nM, and 1 nM in triplicate. Determination of $\alpha 1$ affinity was done in a competition experiment with the radioligand [³H]prazosin at a final concentration of 0.4 nM.

Mitogenesis Assay. The mitogenesis experiments were done with a CHO dhfr⁻ cell line stably transfected with the human dopamine D3 receptor according to literature.^{20,40,41} In brief, cells were grown in DMEM supplemented with dialyzed fetal calf serum, amino acid supplement, L-glutamine, penicillin G, and streptomycin at 37 °C under a humidified atmosphere of 5% CO₂–95% air at a density of 10 000 cells/well. After 72 h the growth medium was removed and the cells were rinsed twice with serum free medium. Incubation was started by adding eight different concentrations of the test compounds as quadruplicates (with a final concentration of 0.01–10 000 nM) diluted in 10 μL of sterile water to each well containing 90 μL serum free medium. After incubation for 16–18 h, 0.02 μCi of [³H]thymidine (specific activity 25 Ci/mmol, Amersham Biosciences) in 10 μL of serum free medium was added to each well for 4 h at 37 °C. Finally, cells were trypsinized and harvested onto GF/C filters using an automated cell harvester. Filters were washed five times with ice-cold PBS buffer and counted in a microplate scintillation counter.

Data Analysis. The resulting competition curves of the receptor binding experiments were analyzed by nonlinear regression using the algorithms in PRISM 3.0 (GraphPad Software, San Diego, CA). The data were initially fit using a sigmoid model to provide a slope coefficient (n_H) and an IC₅₀ value, representing the concentration corresponding to 50% of maximal inhibition. Data were then calculated for a one-site ($n_H \sim 1$) or a two-site model ($n_H < 1$) depending on the slope factor. IC₅₀ values were transformed to K_i values or to $K_{i\text{ high}}$ and $K_{i\text{ low}}$ in the fact when a two-site model was preferred after fitting mono- and biphasic curves according to the equation of Cheng and Prusoff.⁴²

Experimental data resulting from the mitogenesis assay were each normalized and then combined to get a mean curve. Nonlinear regression analysis of this curve provided an EC₅₀ value indicating the concentration of the test compound which induced half of the maximal uptake of [³H]thymidine. The top value of the curve represented the maximal intrinsic activity which could be correlated to the effect of the full agonist quinpirole (100%).

Modeling. To characterize the geometry and energy of the hydrogen-bond interaction of the water–(S)-1 complex and to evaluate the strength of the interaction in comparison to other hydrogen-bond complexes, we employed a validated quantum-chemical method reported by Rablen et al. for our calculations.³⁵

Treatment of the electron correlation with either density functional theory (B3LYP) or second-order Møller–Plesset theory (MP2) was demonstrated to yield similar and reliable interaction energies, when using an appropriate basis set. Thus, due to the more efficient use of computing resources and the smaller basis set superposition error (BSSE) reported for the DFT method, we applied Becke's three parameter hybrid method using the correlation functional of Lee, Yang, and Parr (B3LYP). Moreover, Rablen et al. demonstrated that structure optimization with a 6-31+G(d(X+),p) basis set and subsequent single point calculation using a 6-31++G(2d-(X+),p) basis set achieves the desired level of accuracy in dipole moment and dimerization energy of water. Thereby, an additional set of diffuse d polarization functions, referred to as "X+", are included only on atoms having lone pairs. The starting geometry of water in complex with (S)-1 was derived from the optimized structure of the pyridine–water complex reported in the original publication. To facilitate the comparison of our results with the geometry and energy data previously reported, all calculations were performed in exact compliance with the original method and the homogeneity with the literature data was proven by sample calculations.

Acknowledgment. The authors wish to thank Dr. H. H. M. Van Tol (Clarke Institute of Psychiatry, Toronto), Dr. J.-C. Schwartz, and Dr. P. Sokoloff (INSERM, Paris) as well as J. Shine (The Garvan Institute of Medical Research, Sydney) for providing dopamine D4, D3, and D2 receptor expressing cell lines, respectively. This work was supported by the BMBF and Fonds der Chemischen Industrie.

Supporting Information Available: X-ray crystallographic data of (5R)-9, elemental analyses, and IR spectroscopic data. This material is available free of charge via the Internet at <http://pubs.acs.org>.

References

- (1) Sibley, D. R.; Monsma, F. J., Jr. Molecular biology of dopamine receptors. *Trends Pharmacol. Sci.* **1992**, *13*, 61–69.
- (2) Sokoloff, P.; Giros, B.; Martres, M. P.; Bouthenet, M. L.; Schwartz, J. C. Molecular cloning and characterization of a novel dopamine receptor (D3) as a target for neuroleptics. *Nature* **1990**, *347*, 146–151.
- (3) Dikeos, D. G.; Papadimitriou, G. N.; Avramopoulos, D.; Karadima, G.; Daskalopoulou, E. G.; Souery, D.; Mendlewicz, J.; Vassilopoulos, D.; Stefanis, C. N. Association between the dopamine D3 receptor gene locus (DRD3) and unipolar affective disorder. *Psychiatr. Genet.* **1999**, *9*, 189–195.
- (4) Richtand, N. M.; Woods, S. C.; Berger, S. P.; Strakowski, S. M. D3 dopamine receptor, behavioral sensitization, and psychosis. *Neurosci. Biobehav. Rev.* **2001**, *25*, 427–443.
- (5) Joyce, J. N.; Ryo, H. L.; Beach, T. B.; Caviness, J. N.; Stacy, M.; Gurevich, E. V.; Reiser, M.; Adler, C. H. Loss of response to levodopa in Parkinson's disease and co-occurrence with dementia: role of D3 and not D2 receptors. *Brain Res.* **2002**, *955*, 138–152.
- (6) Bezard, E.; Ferry, S.; Mach, U.; Stark, H.; Leriche, L.; Boraud, T.; Gross, C.; Sokoloff, P. Attenuation of levodopa-induced dyskinesia by normalizing dopamine D3 receptor function. *Nat. Med.* **2003**, *9*, 762–767.
- (7) Pilla, M.; Perachon, S.; Sautel, F.; Garrido, F.; Mann, A.; Wermuth, C. G.; Schwartz, J. C.; Everitt, B. J.; Sokoloff, P. Selective inhibition of cocaine-seeking behaviour by a partial dopamine D3 receptor agonist. *Nature* **1999**, *400*, 371–375.
- (8) Palczewski, K.; Kumasaka, T.; Hori, T.; Behnke, C. A.; Motoshima, H.; Fox, B. A.; Le Trong, I.; Teller, D. C.; Okada, T.; Stenkamp, R. E.; Yamamoto, M.; Miyano, M. Crystal structure of rhodopsin: A G protein-coupled receptor. *Science* **2000**, *289*, 739–745.
- (9) Boeckler, F.; Lanig, H.; Gmeiner, P. Modeling the Similarity and Divergence of Dopamine D2-like Receptors and Identification of Validated Ligand-Receptor Complexes. *J. Med. Chem.* **2005**, *48*, 694–709.
- (10) Boeckler, F.; Ohnmacht, U.; Lehmann, T.; Utz, W.; Hübner, H.; Gmeiner, P. CoMFA and CoMSIA Investigations Revealing Novel Insights into the Binding Modes of Dopamine D3 Receptor Agonists. *J. Med. Chem.* **2005**, *48*, 2493–2508.

- (11) Lehmann, T.; Hübner, H.; Gmeiner, P. Dopaminergic 7-amino-tetrahydroindolizines: ex-chiral pool synthesis and preferential D3 receptor binding. *Bioorg. Med. Chem. Lett.* **2001**, *11*, 2863–2866.
- (12) Gmeiner, P.; Lerche, H. New and efficient synthesis of 5,6,7,8-tetrahydroindolizidines. Application to the synthesis of pharmacologically relevant chiral amino derivatives from L-asparagine. *Heterocycles* **1990**, *31*, 9–12.
- (13) Dijkstra, D.; Rodenhuis, N.; Vermeulen, E. S.; Pugsley, T. A.; Wise, L. D.; Wikstrom, H. V. Further characterization of structural requirements for ligands at the dopamine D(2) and D(3) receptor: exploring the thiophene moiety. *J. Med. Chem.* **2002**, *45*, 3022–3031.
- (14) Tamura, Y.; Minamikawa, J.; Ikeda, M. O-mesitylenesulfonyl-hydroxylamine and related compounds—powerful aminating reagents. *Synthesis* **1977**, 1–17.
- (15) Brown, R. F. C.; Eastwood, F. W.; Fallon, G. D.; Lee, S. C.; McGeary, R. P. The pyrolytic rearrangement of 1-alkynoyl-3-methylpyrazoles: synthesis of pyrazolo[1,5-a]pyridin-5-ols and related compounds. *Aust. J. Chem.* **1994**, *47*, 991–1007.
- (16) Olah, G. A.; Narang, S. C. Iodotrimethylsilane, a versatile synthetic reagent. *Tetrahedron* **1982**, *38*, 2225–2277.
- (17) Dess, D. B.; Martin, J. C. A useful 12-I-5 triacetoxypiperidine (the Dess–Martin periodinane) for the selective oxidation of primary or secondary alcohols and a variety of related 12-I-5 species. *J. Am. Chem. Soc.* **1991**, *113*, 7277–7287.
- (18) Hübner, H.; Haubmann, C.; Utz, W.; Gmeiner, P. Conjugated enynes as nonaromatic catechol bioisosteres: synthesis, binding experiments, and computational studies of novel dopamine receptor agonists recognizing preferentially the D(3) subtype. *J. Med. Chem.* **2000**, *43*, 756–762.
- (19) Hayes, G.; Biden, T. J.; Selbie, L. A.; Shine, J. Structural subtypes of the dopamine D2 receptor are functionally distinct: expression of the cloned D2A and D2B subtypes in a heterologous cell line. *Mol. Endocrinol.* **1992**, *6*, 920–926.
- (20) Sokoloff, P.; Andrieux, M.; Besancon, R.; Pilon, C.; Martres, M. P.; Giros, B.; Schwartz, J. C. Pharmacology of human dopamine D3 receptor expressed in a mammalian cell line: comparison with D2 receptor. *Eur. J. Pharmacol.* **1992**, *225*, 331–337.
- (21) Asghari, V.; Sanyal, S.; Buchwaldt, S.; Paterson, A.; Jovanovic, V.; Van Tol, H. H. Modulation of intracellular cyclic AMP levels by different human dopamine D4 receptor variants. *J. Neurochem.* **1995**, *65*, 1157–1165.
- (22) Schneider, C. S.; Mierau, J. Dopamine autoreceptor agonists: resolution and pharmacological activity of 2,6-diaminotetrahydrobenzothiazole and an aminothiazole analogue of apomorphine. *J. Med. Chem.* **1987**, *30*, 494–498.
- (23) van Vliet, L. A.; Rodenhuis, N.; Dijkstra, D.; Wikstrom, H.; Pugsley, T. A.; Serpa, K. A.; Meltzer, L. T.; Heffner, T. G.; Wise, L. D.; Lajiness, M. E.; Huff, R. M.; Svensson, K.; Sundell, S.; Lundmark, M. Synthesis and pharmacological evaluation of thiopyran analogues of the dopamine D₃ receptor-selective agonist (4aR,10bR)-(+)-trans-3,4,4a,10b-tetrahydro-4-n-propyl-2H,5H-[1]benzopyrano[4,3-b]-1,4-oxazin-9-ol (PD 128907). *J. Med. Chem.* **2000**, *43*, 2871–2882.
- (24) Wikstrom, H.; Andersson, B.; Sanchez, D.; Lindberg, P.; Arvidsson, L. E.; Johansson, A. M.; Nilsson, J. L.; Svensson, K.; Hjorth, S.; Carlsson, A. Resolved monophenolic 2-aminotetralins and 1,2,3,4,4a,5,6,10b-octahydrobenzo[*l*]quinolines: structural and stereochemical considerations for centrally acting pre- and postsynaptic dopamine-receptor agonists. *J. Med. Chem.* **1985**, *28*, 215–225.
- (25) Titus, R. D.; Kornfeld, E. C.; Jones, N. D.; Clemens, J. A.; Smalstig, E. B.; Fuller, R. W.; Hahn, R. A.; Hynes, M. D.; Mason, N. R.; Wong, D. T.; Foreman, M. M. Resolution and absolute configuration of an ergoline-related dopamine agonist, trans-4,4a,5,6,7,8,8a,9-Octahydro-5-propyl-1H(or 2H)-pyrazolo[3,4-g]-quinoline. *J. Med. Chem.* **1983**, *26*, 1112–1116.
- (26) Gmeiner, P.; Mierau, J.; Hofner, G. Enantiomerically pure aminoindolizines: bicyclic ergoline analogues with dopamine autoreceptor activity. *Arch. Pharm. (Weinheim)* **1992**, *325*, 57–60.
- (27) Bergauer, M.; Hübner, H.; Gmeiner, P. Practical ex-chiral-pool methodology for the synthesis of dopaminergic tetrahydroindoles. *Tetrahedron* **2004**, *60*, 1197–1204.
- (28) Mierau, J.; Schneider, F. J.; Ensinger, H. A.; Chio, C. L.; Lajiness, M. E.; Huff, R. M. Pramipexole binding and activation of cloned and expressed dopamine D2, D3 and D4 receptors. *Eur. J. Pharmacol.* **1995**, *290*, 29–36.
- (29) Chio, C. L.; Lajiness, M. E.; Huff, R. M. Activation of heterologously expressed D3 dopamine receptors: comparison with D2 dopamine receptors. *Mol. Pharmacol.* **1994**, *45*, 51–60.
- (30) Brenk, R.; Naerum, L.; Gradler, U.; Gerber, H. D.; Garcia, G. A.; Reuter, K.; Stubbs, M. T.; Klebe, G. Virtual screening for submicromolar leads of tRNA-guanine transglycosylase based on a new unexpected binding mode detected by crystal structure analysis. *J. Med. Chem.* **2003**, *46*, 1133–1143.
- (31) Sung, B. J.; Hwang, K. Y.; Jeon, Y. H.; Lee, J. I.; Heo, Y. S.; Kim, J. H.; Moon, J.; Yoon, J. M.; Hyun, Y. L.; Kim, E.; Eum, S. J.; Park, S. Y.; Lee, J. O.; Lee, T. G.; Ro, S.; Cho, J. M. Structure of the catalytic domain of human phosphodiesterase 5 with bound drug molecules. *Nature* **2003**, *425*, 98–102.
- (32) Okada, T.; Fujiyoshi, Y.; Silow, M.; Navarro, J.; Landau, E. M.; Shichida, Y. Functional role of internal water molecules in rhodopsin revealed by X-ray crystallography. *Proc. Natl. Acad. Sci. U.S.A.* **2002**, *99*, 5982–5987.
- (33) Li, J.; Edwards, P. C.; Burghammer, M.; Villa, C.; Schertler, G. F. Structure of bovine rhodopsin in a trigonal crystal form. *J. Mol. Biol.* **2004**, *343*, 1409–1438.
- (34) Okada, T.; Sugihara, M.; Bondar, A. N.; Elstner, M.; Entel, P.; Buss, V. The retinal conformation and its environment in rhodopsin in light of a new 2.2 Å crystal structure. *J. Mol. Biol.* **2004**, *342*, 571–583.
- (35) Rablen, P. R.; Lockman, J. W.; Jorgensen, W. L. Ab Initio Study of Hydrogen-Bonded Complexes of Small Organic Molecules with Water. *J. Phys. Chem. A* **1998**, *102*, 3782–3797.
- (36) Angeles, A. R.; Neagu, I.; Birzin, E. T.; Thornton, E. R.; Smith, A. B., 3rd; Hirschmann, R. Synthesis and binding affinities of novel SRIF-mimicking β-D-glucosides satisfying the requirement for a π-cloud at C1. *Org. Lett.* **2005**, *7*, 1121–1124.
- (37) Lundstrom, K.; Turpin, M. P.; Large, C.; Robertson, G.; Thomas, P.; Lewell, X. Q. Mapping of dopamine D3 receptor binding site by pharmacological characterization of mutants expressed in CHO cells with the Semliki Forest virus system. *J. Recept. Signal Transduction Res.* **1998**, *18*, 133–150.
- (38) Lowry, O. H.; Rosebrough, N. J.; Farr, A. L.; Randall, R. J. Protein measurement with the Folin phenol reagent. *J. Biol. Chem.* **1951**, *193*, 265–275.
- (39) Heindl, C.; Hübner, H.; Gmeiner, P. Ex-chiral pool synthesis and receptor binding studies of 4-substituted prolinol derivatives. *Tetrahedron: Asymmetry* **2003**, *14*, 3141–3152.
- (40) Hübner, H.; Kraxner, J.; Gmeiner, P. Cyanoindole derivatives as highly selective dopamine D(4) receptor partial agonists: solid-phase synthesis, binding assays, and functional experiments. *J. Med. Chem.* **2000**, *43*, 4563–4569.
- (41) Bettinetti, L.; Schlotter, K.; Hübner, H.; Gmeiner, P. Interactive SAR studies: rational discovery of super-potent and highly selective dopamine D3 receptor antagonists and partial agonists. *J. Med. Chem.* **2002**, *45*, 4594–4597.
- (42) Cheng, Y.; Prusoff, W. H. Relationship between the inhibition constant (K₁) and the concentration of inhibitor which causes 50 per cent inhibition (I₅₀) of an enzymatic reaction. *Biochem. Pharmacol.* **1973**, *22*, 3099–3108.

JM0503805